Pressure induced magnetic, electronic and mechanical properties of SmX (X = Se, Te)

2009 J. Phys.: Condens. Matter 21 436011

(http://iopscience.iop.org/0953-8984/21/43/436011)

J. Phys.: Condens. Matter **21** (2009) 436011 (10pp) doi:10.1088/0953-8984/21/43/436011

Pressure induced magnetic, electronic and mechanical properties of SmX (X = Se, Te)

D C Gupta and Subhra Kulshrestha

Condensed Matter Theory Group, School of Studies in Physics, Jiwaji University, Gwalior-474 011 (MP), India

E-mail: sosfizix@yahoo.co.in and subhrfizix@yahoo.co.in

Received 8 July 2009, in final form 18 September 2009
Published 8 October 2009
Online at stacks.iop.org/JPhysCM/21/436011

Abstract

The magnetic, structural, elastic and electronic properties of Sm–chalcogenides in the stable $Fm\bar{3}m$ and high pressure $Pm\bar{3}m$ phase have been analyzed using an *ab initio* pseudo-potential method with a spin-polarized GGA based on exchange–correlation energy optimization, as implemented in SIESTA code. The magnetic phase stability has been determined from the total energy calculations in non-magnetic and magnetic phases, which clearly indicate that at ambient and high pressures, these compounds are ferromagnetically stable. Also, the Sm ion is described in both five and six localized f electrons. Under compression the Sm chalcogenides undergo a first-order transformation from Sm^{2+} to a stable valence state (Sm^{3+}) with delocalization of the 4f electrons into the 5d states of Sm followed by a structural transition from the B1 to the B2 phase. The structural properties namely, equilibrium lattice constant, bulk modulus, its pressure derivative, transition pressure and volume collapse agree well with the experimental results. We have also computed the electronic structure at different volumes.

(Some figures in this article are in colour only in the electronic version)

1. Introduction

Rare-earth compounds (RECs) have attracted experimental [1–16] and theoretical attention [17–28] due to the presence of strongly correlated electrons in them. They possess interesting structural, mechanical, magnetic, magneto-optic and electronic properties which make them candidates for industrial and technological applications. Out of these RECs, samarium mono-chalcogenides SmX (X = S, Se, Te) have been investigated in greater detail, in view of their technological applications [2, 3] in spintronics and spin filtering devices. Synchrotron radiation and x-ray diffraction (XRD) studies on these compounds show that they crystallize in the $Fm\bar{3}m$ (B1) structure and their lattice parameter 'a' increases with increasing anion size [1–3, 8]. These compounds undergo a pressure induced structural transformation from a six-fold coordinated B1 to an eight-fold coordinated $Pm\bar{3}m$ (B2) structure. In addition, it has also been found [1, 3, 6–8] that some of these compounds show an iso-structural valence transition from divalent (2+) to mixed-valent (3+) states due to promotion of highly correlated f electrons into the 5d conduction band states of the Sm ion. These compounds are semiconducting if Sm is divalent and become metallic if its nature is trivalent. The semiconducting SmSe and SmTe have an unusual gap, as the fundamental excitation is f to d. It gives rise to excitation of localized f electrons, which are predominantly of rare-earth d character.

SmSe undergoes a structural phase transformation from the B1 to the B2 phase at 25 GPa [8], while SmTe undergoes the transformation at 11 GPa [3] and 12.9 GPa [8]. This B1 to B2 transition is accompanied by an electronic collapse in the pressure range of 1–50 kbar for SmSe and 1–60 kbar for SmTe [3]. The measurements by Sidorov *et al* [6] on the thermoelectric power and electrical resistance up to 12 GPa have shown an iso-structural transition at 3.4 GPa for SmSe and 5.2 GPa for SmTe, while Tsiok *et al* [7] have measured similar properties up to 9 GPa and reported a valence transition at 2.3 GPa for SmSe and 4.2 GPa for SmTe. Earlier Shchennikov *et al* [4] also measured the pressure dependence of thermoelectric power and resistivity of SmX up to 35 GPa and reported that in the pressure range of 20–35 GPa, the thermoelectric power is almost independent of the pressure, this being attributed to a passage of samarium ions into the stable trivalent state. In the last decade, Bihan, *et al* [8] measured a similar transition at 3–9 GPa for SmSe and 6–8 GPa for SmTe using a synchrotron radiation source. The

band structure of Sm-compounds has been investigated by Farberovich [17] using the APW method without spin effect. To the best of our knowledge, no theoretical studies have been performed on the structural and elastic properties of these compounds under high pressure.

The phase transition properties of SmTe have been computed by SIESTA within LDA [28] and the results obtained were in good agreement with the experimental data [5, 8] and better than those obtained by others [19]. This encouraged us to take up the present study with the spin-polarized generalized gradient approximation (GGA) because these materials are strongly correlated in nature and hence spin is considered for studying magnetic properties.

Herein, we present our understanding of the possible semiconductor–metal transitions and magnetic orderings in these rare-earth mono-chalcogenides by performing self-consistent calculations of the magnetic, structural and electronic properties of SmSe and SmTe at ambient conditions (B1), as well as at high pressure in the B2 phase, using SIESTA with the spin-polarized GGA by computing the lattice parameter, bulk modulus and its first-order pressure derivative, second-order elastic constants (SOECs) and their combinations, phase transition pressure (P_T), equation of state (EOS) and volume collapse at P_T. We have described the essential theory and methodology of the computation in the next section followed by a discussion on the results obtained. The paper is finally concluded in section 4.

2. Theory and method of calculation

The present ground state calculations are based on the first-principles pseudo-potential method within the density functional formalism and spin-polarized GGA using the Perdew, Burke, and Ernzerhof functional [29] for the exchange–correlation energy and standard norm conserving pseudo-potential of Troullier–Martins [30] in relativistic form. All calculations are performed by using the SIESTA code which is appropriate for electronic structure calculations of large systems ([31] and the references therein). In SmSe and SmTe, the Sm atom occupies (0, 0, 0) while the Se and Te atoms are at (0.5, 0.5, 0.5) positions. The ground state valence configuration of Sm ($5d^0\ 4f^6$), Se ($4s^2\ 4p^4\ 4d^0$) and Te ($5s^2\ 5p^4\ 5d^0$), respectively have been used for the present calculations under ambient conditions. Under compression, the 4f states of samarium ion fluctuate to 5d states showing an intermediate valence transition from Sm^{2+} ($Sm^{2+}{\cdot}Se^{2-}/Te^{2-}$) to a stable valence state ($Sm^{3+}{\cdot}Se^{2-}/Te^{2-} + 1e^-$). Although, a mixed-valent transition is observed the system still remains stable in the B1 phase. To study this transition, we have generated pseudo-potentials for divalent Sm with the $6s^2\ 5p^6\ 5d^0\ 4f^6$ valence configuration and for trivalent Sm with the $6s^2\ 5p^6\ 5d^1\ 4f^5$ valence configuration. This forms the basis set for our calculation. Double-ζ with perturbative polarization for Sm 6s, Se 4s and Te 5s states and double-ζ for Sm 5p, 5d, 4f, Se 4p and Te 5p states have been used. To solve the self-consistent Kohn–Sham equations, we have performed a convergence test for mesh cut-off and k-point up to a energy difference of 25 meV. We have used a basis of plane waves up to a kinetic energy of 124.2 and 109.6 Ryd for SmSe and SmTe, respectively. We have used a $10 \times 10 \times 10$ k-grid (1000 k points) in the Brillouin-zone (BZ). The cut-off radius used for the pseudo-potential for Sm is 3.06, 4.00, 3.06 and 3.06 Bohr for the 6s, 5p, 5d and 4f states, respectively. For Se, we used 3.56 Bohr for the 4s state and 2.35 Bohr for the 4p state while for Te, we used 3.56 Bohr for the 5s state and 2.35 Bohr for the 5p state. All the atoms are allowed to relax until a force tolerance of 0.01 eV $Å^{-1}$ and stress tolerance of 0.01 GPa is reached, while restricting their structure to be cubic only.

3. Results and discussion

3.1. Magnetic state stability

We have carried out self-consistent calculations of the total energy in the non-magnetic (NM) and magnetic (M) states in the B1 phase. We have performed both non-spin- and spin-polarized band-structure calculations. The values of total energy computed self-consistently in the NM and M states in the B1 phase were fitted to Murnaghan's equation of state [32] in order to obtain the pressure–volume relationship.

$$\frac{V}{V_0} = \left(1 + \frac{B_0'}{B_0} P\right)^{-\frac{1}{B_0'}}. \tag{1}$$

Here, $B_0(=-V(\partial P/\partial V)_T)$ is the equilibrium bulk modulus, $B_0'(=(\partial B_0/\partial P)_T)$ its first-order pressure derivative and $P(=-\partial E/\partial V)$ is a pressure which is defined as the negative derivative of the total energy.

The Gibb's free energy has been calculated as a function of pressure. The variation of total energy with cell volume for non-magnetic and magnetic states in the B1 phase for Sm-compounds is shown in figures 1 and 2. It is seen from these figures that the non-magnetic-to-magnetic transition does not occur in these compounds (the curves for NM and M states do not intersect). The energy remains lower in the magnetic phase. Therefore, the ferromagnetic state is more stable than the non-magnetic state at ambient as well as at high pressures. The equilibrium cell volume in the magnetic state at ambient pressure is estimated to be 405.93 and 491.61 au^3 for SmSe and SmTe, respectively. The calculated equilibrium lattice parameters 'a' are 6.22 and 6.63 Å. These values are comparable to the experimentally observed values of 6.20 and 6.60 Å [8] for SmSe and SmTe, respectively.

3.2. Phase transition properties

For computing the phase transition properties, we have performed self-consistent calculations of the total energy at room temperature as a function of volume in all the phases. The calculated results in the B1 and B2 phases are plotted in figures 3 and 4. It is seen from these figures that these compounds are stable in the B1 phase at ambient conditions and undergo an iso-structural valence transition from the Sm^{2+} to mixed-valent Sm^{3+} state followed by a more compressed B2 phase. This is consistent with experiments [2, 3, 6–8].

Under ambient conditions, the energy of the B1 phase with divalent Sm is less than that of trivalent Sm in the same phase.

Table 1. The values of lattice parameter (a), bulk modulus (B_0) and its pressure derivative (B_0') of SmSe and SmTe in the B1 and B2 phases.

	a (Å)			B_0 (GPa)			B_0'
Solids	Present	Expt. [5, 8]	Others [19]	Present	Expt. [5, 8]	Others [19]	Present
				B1 phase			
SmSe	6.22	6.20	6.19	43.12	40 ± 5	43.9	3.30
SmTe	6.63	6.60	6.59	43.46	40 ± 5	37.6	3.74
				B2 phase			
SmSe	3.88	—	—	71.09	—	—	3.77
SmTe	3.37	—	—	95.04	—	—	2.88

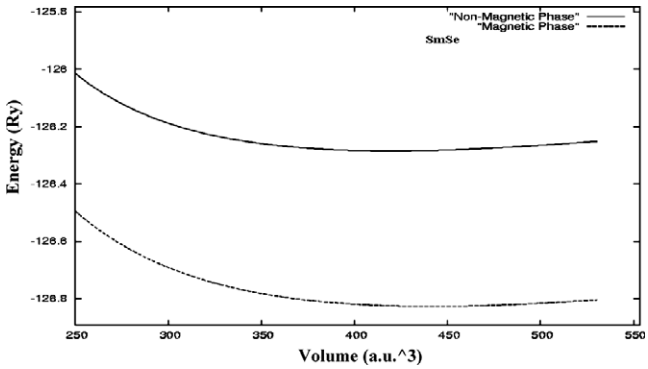

Figure 1. Total energy versus cell volume for both the NM and M states of the B1 phase for SmSe.

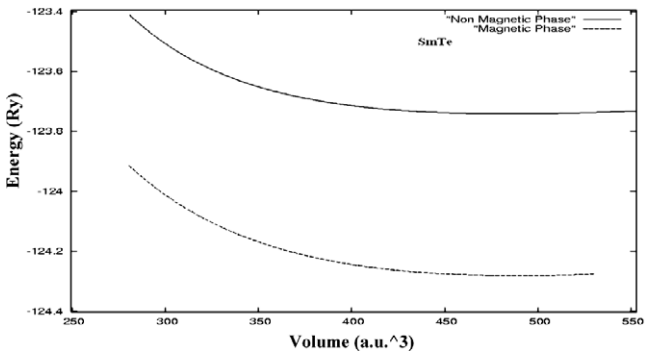

Figure 2. Total energy versus cell volume for both the NM and M states of the B1 phase for SmTe.

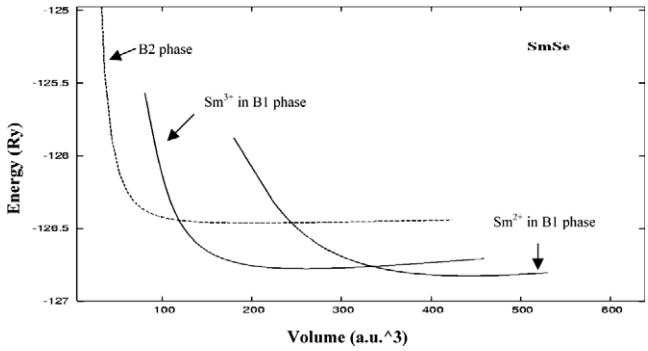

Figure 3. The variation of energy (Ryd/unit cell/atom) versus volume for various structures of SmSe.

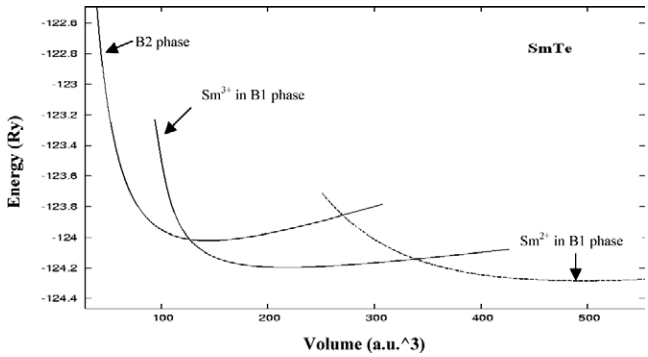

Figure 4. The variation of energy (Ryd/unit cell/atom) versus volume for various structures of SmTe.

On further compression, beyond the B1 → B2 transformation, the energy of the B2 phase becomes lower compared to that of the B1 phase which fulfils the required criterion for relative stability of the competitive phases. It is clear from figures 3 and 4 that convergence occurs at a value close to the experimental lattice constant. The correct description of the lattice constant confirms that the interactions considered in the present computation and the process of the self-consistent field approach are capable of correctly predicting the minimum free energy (total energy at room temperature) of these compounds in the parent (B1) phase.

The calculated values of total energy are fitted to Murnaghan's equation of state [32] to determine the ground state properties, such as the equilibrium lattice parameter, the bulk modulus and its pressure derivative. These results are presented in table 1 and compared with available experimental [5, 8] and other theoretical [19] data.

The calculated value of the equilibrium lattice constant is overestimated by 0.32% for SmSe and 0.45% for SmTe with respect to the corresponding measured value. This over estimation of these values lies within the limits of DFT with GGA. Under ambient conditions, SmSe and SmTe crystallize in the rock-salt (B1) phase with a bulk modulus (B_0 = 43.12, 43.46 GPa), respectively which is found to be smaller than the values (B_0 = 71.09, 95.04 GPa, respectively) in the compressed B2 phase. The values of the bulk modulus compare well with experimental data [5, 8]. The values of pressure derivative of bulk modulus are of academic interest at present due to non-availability of measured data.

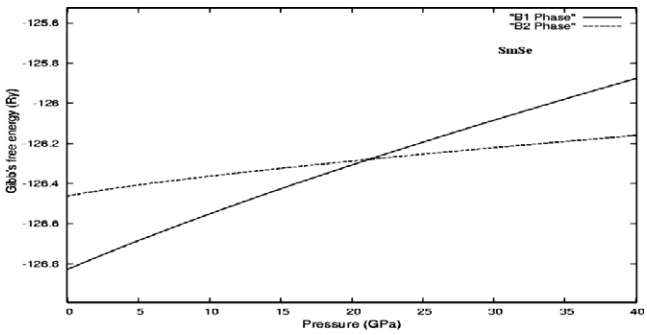

Figure 5. Variation of Gibb's free energy with pressure for SmSe.

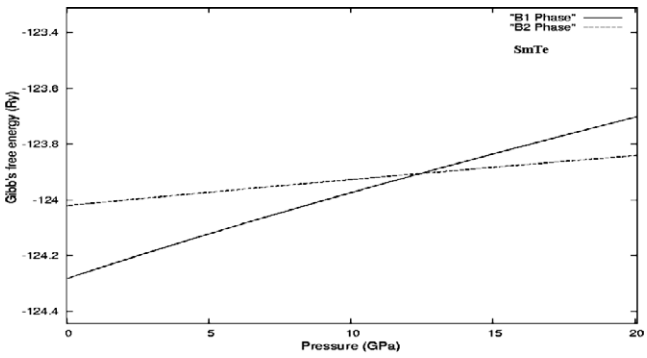

Figure 6. Variation of Gibb's free energy with pressure for SmTe.

To determine the transition pressure, the Gibb's free energy at room temperature in different B1 and hypothetical phases can be expressed as

$$G_{\mathrm{B1}} = E_{\mathrm{B1}} + PV_{\mathrm{B1}} \qquad \text{and} \qquad G_{\mathrm{Hypo}} = E_{\mathrm{Hypo}} + PV_{\mathrm{Hypo}}. \tag{2}$$

It is known that Sm has partially localized f states which delocalize under pressure well before the B1 → B2 transition. Hence, in the present study, the fluctuation of 4f electrons to 5d states of Sm for both the compounds has been studied. The variation of the Gibb's free (GF) energy for both SmSe and SmTe in the Sm^{2+} and mixed valence Sm^{3+} states reveals their equality at 3.87 and 7.1 GPa (not shown in figures), resulting in transformation of semiconducting Sm^{2+} into a mixed-valent state, which shows closer agreement with the available measured data [8] on SmSe (3–9 GPa) and SmTe (6–8 GPa). Beyond this pressure, these compounds remain stable in the B1 phase with mixed-valent i.e., a stable valence state of Sm because the GF energy in this state is lower as compared to the energy of its divalent state. The variation of GF energy in the B1 and B2 phases with pressure is shown in figures 5 and 6. It may be seen from these figures that the GF energy in the parent (B1) phase is minimum at ambient conditions and remains minimum up to 21.39 GPa for SmSe and 12.63 GPa for SmTe. At 21.4 and 12.64 GPa, the GF energy in both the phases becomes equal, showing that both the phases are in equilibrium at this pressure and hence the structural phase transformation in SmSe and SmTe occurs at this point. On further increasing the pressure, the

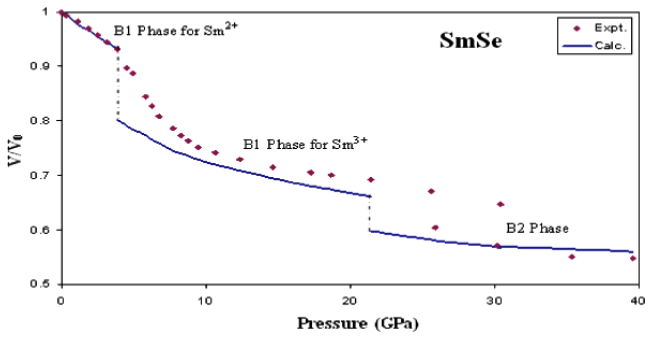

Figure 7. Phase diagram of SmSe. The calculated values (solid line) are compared with experimental data (diamonds) [8].

GF energy minimizes in the B2 phase as compared to that in B1 phase, i.e., the B2 phase becomes stable with more lower GF energy. These values of free energy have been used to compute the Gibb's free energy difference (ΔG) in the B1 and B2 phases to compute the phase transition pressure (P_{T}). The values of the ratio of volumes at high pressure ($V(P)$) to the volume at ambient conditions ($V(0)$) has been computed and plotted in figures 7 and 8 to obtain the equation of state and the volume collapse at P_{T} ($\Delta V(P_{\mathrm{T}})/V(0)$). This equation of state has been used to understand the mechanism from semiconductor to metallization in these compounds. The values of phase transition properties are presented in table 2 along with measured data [3–8] and the theoretical values computed by others [18, 19].

It is clear from figure 7 that the volume of SmSe decreases smoothly up to 3.87 GPa. At this pressure, an abrupt decline in volume is observed. This discontinuity may be associated with a first-order iso-structural valence transformation which is responsible for an electronic transition in these compounds. After 3.87 GPa, the volume again decreases smoothly. At 21.4 GPa, another abrupt change of volume has been observed, which is associated with the structural phase transformation in SmSe from the B1 → B2 phase and thereafter no other transformation is observed because no abrupt decline in volume is found up to 90 GPa. A similar trend of transformation is found in SmTe as depicted in figure 8, except that the transition occurs at different magnitudes of pressure, i.e., at 7.1 GPa for the electronic transition and at 12.64 GPa for the structural phase transformation. The values of the discontinuities in reduced volume at the transition pressure ($\Delta V(P_{\mathrm{T}})/V(0)$) are reported in table 2 along with available experimental data.

3.3. Elastic properties

Elastic constants are the measure of strength of a crystal under an externally applied stress. For small strains Hooke's law is obeyed and the crystal energy E is a quadratic function of strain [33]. Thus, for obtaining the total minimum energy to calculate the SOECs, the crystal is strained with all the internal parameters relaxed. Consider a symmetric 3 × 3 non-rotating strain tensor (which has matrix elements ε_{ij} ($i, j = 1, 2$ and

Table 2. The calculated values of the phase transition pressure (P_T in GPa), volume collapse at P_T ($\Delta V(P_T)/V(0)$), energy of structures at zero pressure with respect to the rock-salt phase ($\Delta G = G_{Hypo} - G_{(B1)}$ in Ryd/unit cell/atom) and the equilibrium volume (V_0, in Å^3) for SmSe and SmTe.

	Sm^{2+} to Sm^{3+} (B1 phase)		B1 → B2		
Properties	SmSe	SmTe	SmSe	SmTe	Reference
P_T	3.87	7.1	21.4	12.64	Present work
	4[a], 3.4[b], 3–9[c], 2.6–4[d]	2–8[a], 5.2[b], 6–8[c], 4.6–7.5[d]	25[c]	11[e], 12.9[c]	Expt.
	3.3	6.2	—	—	Others [19]
$\Delta V(P_T)/V(0)$	9.6	8.4	6.4	6.26	Present work
	8[a], 11[c], 7[d]	9[c], 7[d]	6.8	6.8	Expt.
	9.8	8.4	—	—	Others [19]
	B1 phase		B2 phase		
ΔG	0.00	0.00	0.56	0.26	Present work
	60.16	72.85	29.20	19.13	Present work
V_0	59.58	71.87	—	—	Expt. [8]
	59.29	71.54	—	—	Others [18]

[a] Reference [5]. [b] Insulator–metal transition of [6]. [c] Present authors estimated from figures of [8].
[d] Reference [7]. The volume change for SmTe is obtained by extrapolation over the transition range.
[e] Reference [3].

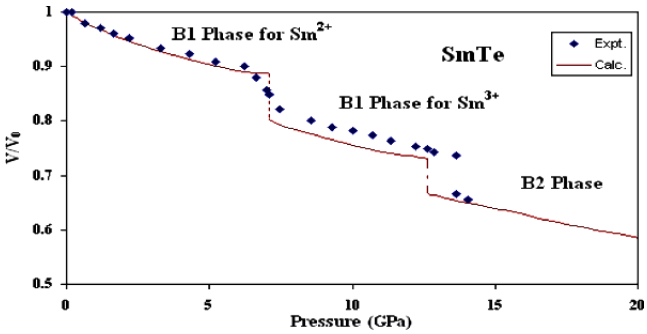

Figure 8. Phase diagram of SmTe. The calculated values (solid line) are compared with experimental data (diamonds) [8].

3)) defined as

$$\varepsilon_{ij} = \begin{pmatrix} e_1 & \frac{e_6}{2} & \frac{e_5}{2} \\ \frac{e_6}{2} & e_2 & \frac{e_4}{2} \\ \frac{e_5}{2} & \frac{e_4}{2} & e_3 \end{pmatrix}. \quad (3)$$

Such a strain transforms the three lattice vectors by defining the unstrained Bravais lattice $\{\mathbf{a}_k, k = 1, 2, \text{and } 3\}$ to the strained vectors $\{\mathbf{a}'_k, k = 1, 2, \text{and } 3\}$ [34] as

$$\mathbf{a}'_k = (\mathbf{I} + \varepsilon)\mathbf{a}_k \quad (4)$$

where $\mathbf{I}$ is defined by its elements, $I_{ij} = 1$ for $i = j$ and 0 for $i \neq j$. Each lattice vector $\mathbf{a}_k$ or $\mathbf{a}'_k$ is a 3×1 matrix. The change in total energy due to above strain (3) is

$$\frac{\Delta E}{V_0} = \frac{E(\{e_i\}) - E_0}{V_0} = \left(1 - \frac{V}{V_0}\right) P(V_0) + \tfrac{1}{2}\left(\sum_{i=1}^{6}\sum_{j=1}^{6} C_{ij} e_i e_j\right) + O(\{e_i^3\}) \quad (5)$$

where V_0 is the volume of the unstrained lattice with E_0 as the total minimum energy at this unstrained volume of the crystal, $P(V_0)$ is the pressure of the unstrained lattice, and V is the new volume of the lattice due to strain in equation (3).

Table 3. Three strain combinations in the strain tensor (equation (3)) for calculating the three elastic constants of cubic structures. The three independent elastic constants C_{11}, C_{12}, and C_{44} for SmSe and SmTe in the parent B1 phase are calculated from the above strains. Symmetry dictates $C_{ij} = C_{ji}$ and all unlisted $C_{ij} = 0$. The strain δ is varied in steps of 0.01 from $\delta = -0.02$ to 0.02. ΔE (equation (5)) is the difference in energy between that of the strained lattice and the unstrained lattice. The equilibrium or unstrained lattice volume is V_0.

Strain	Parameters (unlisted $e_i = 0$)	$\Delta E/V_0$
1	$e_1 = e_2 = \delta, e_3 = (1+\delta)^{-2} - 1$	$3(C_{11} - C_{12})\delta^2$
2	$e_1 = e_2 = e_3 = \delta$	$3(C_{11} + 2C_{12})\delta^2/2$
3	$e_6 = \delta, e_3 = \delta^2(4 - \delta^2)^{-1}$	$C_{44}\delta^2/2$

In equation (5), $C_{ij} = C_{ji}$ due to crystal symmetry [33]. This reduces the elastic stiffness constants, C_{ij}, from 36 to 21 independent elastic constants in equation (5). Further crystal symmetry [33, 34] reduces the number to 9 (C_{11}, C_{12}, C_{13}, C_{23}, C_{22}, C_{33}, C_{44}, C_{55}, C_{66}) for orthorhombic crystals, 6 (C_{11}, C_{12}, C_{13}, C_{33}, C_{44}, C_{66}) for tetragonal crystals, and 3 (C_{11}, C_{12}, C_{44}) for cubic crystals. A proper choice of the set of strains $\{e_i, i = 1, 2, \ldots, 6\}$ leads to a parabolic relationship between $\Delta E/V_0$ ($\Delta E = E - E_0$) and the chosen strain. Such choices for the set $\{e_i\}$ and the corresponding form for ΔE are reported in table 3 for cubic lattices [35]. In the present study the lattice is strained by 0%, ±1%, and ±2% to obtain the total minimum energies $E(V)$ at these strains. These energies and strains have been fitted with the corresponding parabolic equations of $\Delta E/V_0$, as reported in table 3, to yield the required SOECs. While computing these energies all atoms were allowed to relax with the cell shape and volume fixed by the choice of strains $\{e_i\}$.

The strain energy ($\frac{1}{2}C_{ij}e_ie_j$) of a given crystal in equation (5) must always be positive for all possible values of the set $\{e_i\}$; otherwise the crystal would be mechanically unstable. This means that the quadratic form ($\frac{1}{2}C_{ij}e_ie_j$) must be positive definite for all real values of strains unless all the strains are zero. This imposes further restrictions on the

Table 4. Calculated elastic properties (in GPa) except σ, A and ξ (unit free) of SmSe and SmTe in the parent B1 phase.

Parameters	SmSe	SmTe
C_{11}	107.76	108.98
C_{12}	10.8	10.7
C_{44}	21.4	18.3
G	32.23	30.64
E	77.41	74.42
σ	0.20	0.21
A	0.44	0.37
$C_{12} - C_{44}$	−10.6	−7.6
C_S	48.48	49.14
C_L	80.68	78.14
ξ	0.250	0.248

elastic constants C_{ij} depending on the crystal structure. These stability conditions can be determined by standard algebraic methods [36]. For cubic crystal structures such as the B1 phase, the necessary conditions for mechanical stability have been given elsewhere [37] as

$$(C_{11} - C_{12}) > 0, \qquad (C_{11} + 2C_{12}) > 0, \qquad C_{11} > 0, \qquad C_{44} > 0. \tag{6}$$

The elastic constants are determined by applying the strains listed in table 3. $(C_{11} - C_{12})$ is obtained by using the strain combination on the first row of table 3. The computed values of all the elastic constants of SmSe and SmTe in B1 phase are reported in table 4. These values satisfy all the stability conditions of equations (6) and hence we may conclude that these compounds are mechanically stable in the B1 phase.

For a cubic crystal, the shear and stiffness constant C_S and C_L is given by:

$$C_S = (C_{11} - C_{12})/2 \qquad \text{and} \qquad C_L = (C_{11} + C_{12} + 2C_{44})/2. \tag{7}$$

Another important parameter is the Kleinman parameter [38]

$$\xi = \frac{C_{11} + 8C_{12}}{7C_{11} + 2C_{12}} \tag{8}$$

which describes the relative positions of the cation and anion sub-lattices under volume conserving strain distortions for which positions are not fixed by symmetry.

The isotropic bulk and shear modulus for a cubic system are given as

$$B_0 = (C_{11} + 2C_{12})/3 \tag{9}$$

and

$$G = 0.2(C_{11} - C_{12} + 3C_{44}). \tag{10}$$

From the elastic constants C_{11}, C_{12} and C_{44}, two parameters having a substantial and geophysical interest can be examined. They are the elastic anisotropy factor A and the Cauchy's relation defined as

$$A = \frac{2C_{44}}{(C_{11} - C_{12})}. \tag{11}$$

The Cauchy relation $C_{12} - C_{44} = 2P$ (P: pressure) is valid only when all interatomic forces are composed by two-body central interactions under static lattice conditions. At zero pressure, our calculations give negative values of $C_{12} - C_{44}$ (table 4), indicating violation of the Cauchy relation. The value of the Cauchy relation increases on increasing the size of chalcogen atom in the B1 phase, which shows that the non-central character of the forces, implicit in the Cauchy relation, increases when the lattice constant decreases. The negative Cauchy discrepancy is a consequence of the hybridization of the unstable 'f' band. This hybridization may be responsible for the decrease in Sm–Sm distance and thereby to a small value of the elastic constant C_{12}. As regards the elastic anisotropic factor (used in the interpretation of the seismological and shear-wave velocities anisotropy), table 4 shows that these compounds are anisotropic (as 'A' approaches unity the crystal becomes isotropic) having a comparatively large value for it as compared to other materials of the rare-earth family [39, 40].

We have also calculated the Young modulus (E) and the Poisson ratio (σ). These quantities are related to the bulk modulus (B_0) and the shear modulus (G) by the following equations, and their values are reported in table 4.

$$E = \frac{9B_0G}{(3B_0 + G)} \qquad \text{and} \qquad \sigma = \frac{(3B_0 - E)}{6B_0}. \tag{12}$$

At present, no experimental data on the elastic properties is reported in the literature. Future experiments will, however, testify these results. We consider the present elastic constants as a prediction study for these compounds with the hope that our present work will stimulate some other work on these heavy rare-earth compounds.

3.4. Electronic properties

The spin-polarized electronic structure of mixed-valent SmSe and SmTe along the high symmetry directions in the BZ under ambient conditions in the B1 and B2 phases are shown in figures 9(a) and (b). The solid line represents the spin-up band structure (BS) while the dotted line represents the BS in the spin-down channel in the B1 phase. The region around −12 eV for SmSe, and −11 eV for SmTe, is mostly due to the chalcogen s character and the next higher region is due to the chalcogen p character. The region above the Fermi level up to 3 eV is mainly due to unoccupied 5d states of Sm. For the spin-up case, Sm f-like states (cluster of solid lines) can be seen at E_F, showing its metallic nature, while for the spin-down case these states can be seen above the Fermi level (cluster of dotted lines), which hybridize with Sm d-like states, showing a semiconducting nature. In the spin-up case, the interaction of Sm f states and chalcogen p states leads to a mutual repulsion so that the chalcogen p states are pushed to energies above the Fermi level. These chalcogen p states connect with lower states and are responsible for the metallic character of the spin-up BS. Since the Sm f levels are polarized above the Fermi level in the spin-down direction, the same interaction of chalcogen p and Sm f states presses the chalcogen p levels below the Fermi level to open a gap, and produces a semiconducting behavior. The overall nature of bands in the spin-up channel for the parent phase resembles the band structure computed earlier [17].

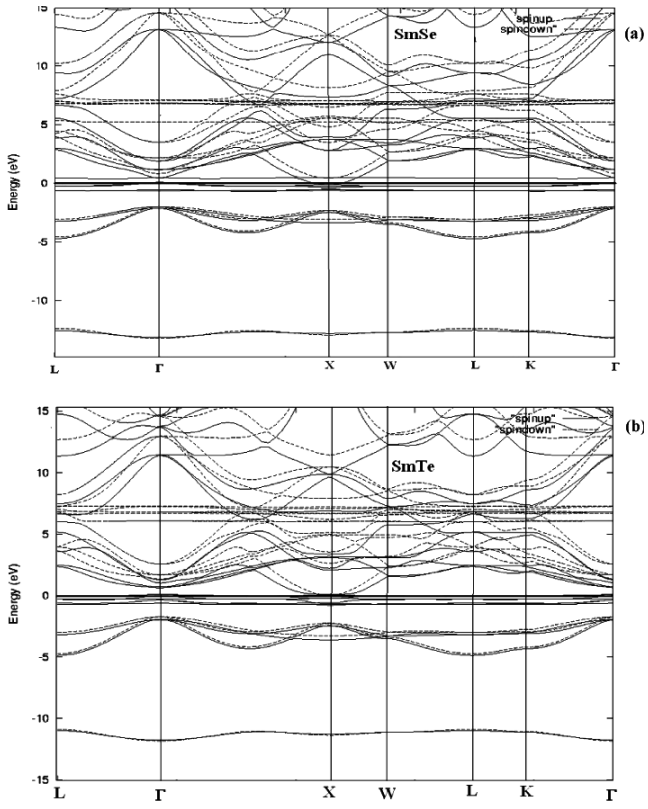

Figure 9. Self-consistent spin-polarized electronic structure calculated for (a) SmSe and (b) SmTe at ambient conditions in the B1 phase. The position of the Fermi level is shown by the solid horizontal line.

The partial density of states (PDOS) of these compounds in the B1 phase at ambient conditions is also shown in figures 10 and 11. From these figures, we may clearly identify the angular-momentum character of the different structures. We emphasize that there are different distinct structures in the density of electronic states separated from each other by distinguishable gaps, confirming the band structures discussed above and showing clearly the contribution of states with spins up and down. We can see from figure 10(a) that the 4s states of Se lie around −12 eV. The next structure localized between −4.9 and −2.0 eV below the zero of energy is dominated by the chalcogen 4p states, which are actively participating in hybridization with Sm 5d states in the spin-up case. Many physical properties of Sm–chalcogenides may be controlled by Sm 5d–4p hybridization (Γ–X direction). This hybridization results in magnetic moments on the chalcogen site and is responsible for the attractive magnetic ordering and transport properties. It may be seen from figure 10(b) that for the spin-up channel, the peaks near the Fermi level are due to Sm 4f states while the same states shift towards the high energy range of 5–6 eV in spin-down channel. The Sm 5d states are dominant above the Fermi level for both the channels. Interestingly, it may be seen from figure 10 that the spin-up and spin-down states of Se s and p and Sm d states lie at the same energy with no separation in between them while Sm f states show separation in their spin-up and spin-down channels. This may be due to the exchange splitting which is necessary in ferromagnetic compounds. A similar behavior of the contribution to the structures is seen in SmTe (figures 11(a) and (b)). The region situated between −12 and −11 eV is due to the 5s states of Te and a second region, ranging from −4.9 to −1.7 eV, is mainly due to the Te (5p) states (figure 11(a)).

It is interesting to note that our calculations on electronic structure in the B1 phase show an energy gap of 2.5 and 1.82 eV (figures 9(a) and (b)) between the p band and the bottom of the conduction band for SmSe and SmTe. It indicates a decrease of the energy gap with an increase in chalcogen size i.e., the 4f bands of Sm approach the p states of the ligands from Se to Te. This increase in the f bandwidth may be interpreted as the interaction of f states of the cation with p states of the anion. The top of the f bands at the Γ point have a tendency to repel each other. It is clear that as the f state approach the p bands at the Γ point, the states in these bands interact with each other. This interband interaction gives rise to an increase in repulsion which results in an increase of the f bandwidth. This effect is stronger in SmTe because the f band is nearest to p band i.e., it contains a considerable admixture of states with p symmetry as compared to SmSe.

To see the effect of high pressure on the electronic structure and phase transformation in these compounds, we

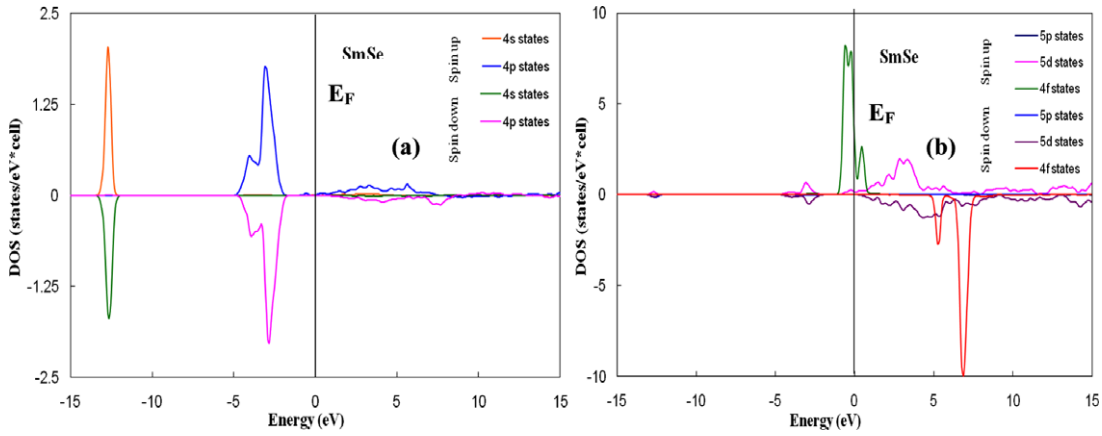

Figure 10. Partial spin-polarized DOS of SmSe in NaCl-B1: (a) the state contributions of the chalcogen (Se) and (b) the state contributions of the samarium (Sm).

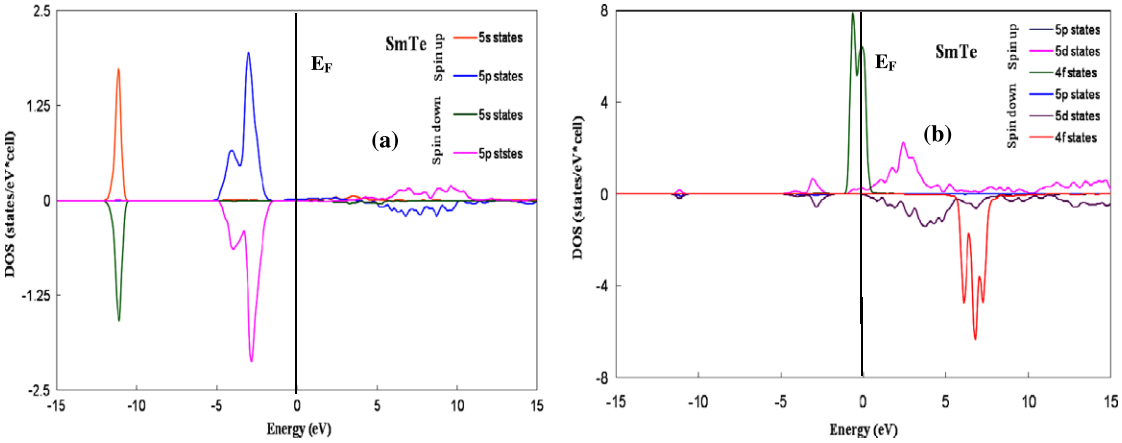

Figure 11. Partial spin-polarized DOS of SmTe in NaCl-B1: (a) the state contributions of the chalcogen (Te) and (b) the state contributions of the samarium (Sm).

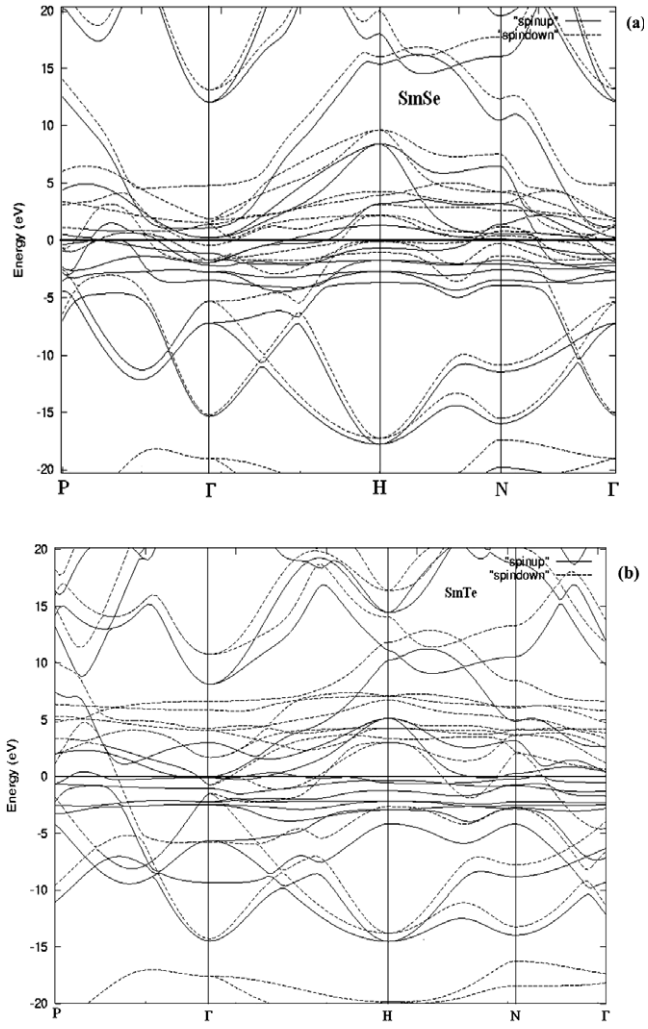

Figure 12. Self-consistent spin-polarized electronic structure calculated for (a) SmSe and (b) SmTe in the B2 phase (just after the B1 → B2 transition).

have also computed the electronic structure in the B2 phase (just after the B1 → B2 transition) for both the compounds and plotted them in figures 12(a) and (b). It may be seen from these figures that the 4f bands of Sm lie close to the Fermi level, which drops down towards the chalcogen p states at the Γ point and overlap with the top of the chalcogen p states at the H point showing metallization. This is because there is a decrease in energy separation between the 4f states and the conduction band edge with an increase in pressure. This is in accordance with the work reported earlier [17]. It may be due to the fractional change in the valence state of Sm during the pressure induced structural transition. Due to the decrease in energy separation with pressure, a fractional delocalization of the 4f states is observed. A similar semiconductor to metal transition has been observed experimentally under pressure [3]. Furthermore, as we increase the pressure, the hybridization of the Sm d states and chalcogen p states increases and the lower energy bands are shifted to the higher energy side. In the spin-down channel the gap between the chalcogen p and Sm d states reduces, while the Sm f states shift to the higher energy side and participate in the bonding with the chalcogen p states. On the other hand, in the case of the spin-down channel the metallic property increases resulting in metallization in the B2 phase.

Spin-polarized self-consistent band-structure calculations have been very successful in calculating and predicting the magnetic moments using the GGA approximation. The calculated values of magnetic moments for SmSe and SmTe are listed in table 5. It is clear from this table that the local and total magnetic moments decrease with an increase in pressure, which is quite natural in magnetic materials. The contribution to the total magnetic moment is mainly due to Sm 4f electrons, while the contribution of the chalcogen atom is almost negligible. But it is interesting to note that the magnetic moment contributed by the chalcogen atom is negative, which indicates that the chalcogen magnetic moment coming from the Se 4p and Te 5p states is anti-parallel to the rare-earth magnetic moment contributed by the Sm 4f states. It is worth mentioning here that these values in both the phases (B1 and B2) are very close to each other and hence we have reported these values in the B1 phase.

Table 5. Total and local magnetic moments (in Bohr magneton μ_B) as function of pressure for SmSe and SmTe in the B1 phase.

Pressure	SmSe			SmTe		
(GPa)	Sm	Se	Total	Sm	Te	Total
0	6.201	−0.201	6.000	6.183	−0.193	5.990
5	6.194	−0.217	5.977	6.180	−0.212	5.968
10	6.189	−0.223	5.966	6.177	−0.232	5.945
15	6.163	−0.228	5.935	6.158	−0.240	5.917
20	6.139	−0.232	5.907	6.135	−0.265	5.870
25	6.130	−0.235	5.895	6.128	−0.280	5.848
30	6.117	−0.261	5.856	6.120	−0.285	5.835

4. Conclusion

In the present paper, we have attempted to provide a unified picture of the crystal properties of these strongly correlated systems. For this purpose, *ab initio* pseudo-potential calculations have been performed to obtain magnetic, iso-structural valence transition, structural phase transition and associated properties, mechanical, electronic, and magnetic properties under pressure by employing spin-polarized GGA as implemented in SIESTA. The present calculations predict that these materials are ferromagnetic in nature and they do not show any magnetic to non-magnetic transition. They show an iso-structural valence transition due to fluctuation of electrons from the f to d states of Sm (($4f^6$, $5d^0$) to ($4f^5$, $5d^1$)) followed by a structural phase transformation from the B1 → B2 phase under pressure. The calculated mechanical properties, namely the lattice constant, bulk modulus and its pressure derivative, SOEC's, Gibb's free energy, transition pressure, EOS and volume collapse at transition pressure are in reasonably good agreement with experimental data and better than other theoretical results. We are not aware of any experimental data for the elastic constants of these compounds in the B1 phases and so our calculations can be used to cover this lack of data for these compounds. The electronic structure has been computed in both the B1 and B2 phases to analyze the effect of f electrons and pressure on the nature of bands in these strongly correlated compounds. The width of the 4f bands is greater for SmTe as compared to SmSe. The calculated local and total magnetic moment decreases with increasing pressure.

Acknowledgments

The authors are grateful to the UGC and DST, New Delhi for financial support. One of us (SK) is also grateful to CSIR, New Delhi for the award of a Senior Research fellowship. Thanks are due to Professor(s) S Auluck and R Prasad for valuable discussions and suggestions during this work. The authors wish to thank to the SIESTA team for providing the code. Thanks are also due to Ms Ellen de Vries and Dr Frank Toolenaar, Philips Research, High Tech Campus 34, 5656 AE Eindhoven, The Netherlands for providing research reports.

References

[1] Rooymans C J M 1968 *Structural Investigations on Some Oxides and Other Chalcogenides at Normal and Very High Pressures* (*Philips Research Reports*) (Eindhoven: Philips)
[2] Chatterjee A, Singh A K and Jayaraman A 1972 *Phys. Rev.* B **6** 2285
[3] Jayaraman A, Singh A K, Chatterjee A and Usha Devi S 1974 *Phys. Rev.* B **9** 2513
[4] Shchennikov V V, Stepanov N N, Smirnov I A and Golubkov A V 1988 *Sov. Phys.—Solid State* **30** 1785
[5] Benedict U and Holzapfel W B 1993 *Handbook on the Physics and Chemistry of Rare Earths* vol 17, ed K A Gschneidner, L Eyring, G H Lander and G R Choppin (Amsterdam: North-Holland)
[6] Sidorov V A, Stepanov N N, Khvostantsev L G, Tsiok O B, Golubkov A V, Oskotski V S and Smirnov I A 1989 *Semicond. Sci. Technol.* **4** 286
[7] Tsiok O B, Sidorov V A, Bredikhin V V and Khvostantsev L G 1991 *Solid State Commun.* **79** 227
[8] Bihan T Le, Darracq S, Heathman S, Benedict U, Mattenberger K and Vogt O 1995 *J. Alloys Compounds* **226** 143
[9] Batlogg B, Kaldis E, Schlegel A and Watcher P 1976 *Phys. Rev.* B **14** 5503
[10] Leger J M, Epain R, Loriers J, Ravot D and Rossat-Mignod J 1983 *Phys. Rev.* B **28** 7125
[11] Leger J M, Ravot D and Rossat-Mignod J 1984 *J. Phys. C: Solid State Phys.* **17** 4935
[12] Mori N, Okayama Y, Takahashi H, Haga Y and Suzuki T 1993 *Physica* B **186–188** 444
[13] Holzapfel W B 1995 *J. Alloys Compounds* **223** 179
[14] Benedict U 1995 *J. Alloys Compounds* **223** 216
[15] Shirotani I, Yamanashi K, Hayashi J, Tanaka Y, Ishimatsu N, Shimomura O and Kikegawa T 2001 *J. Phys.: Condens. Matter* **13** 1939
[16] Shirotani I, Yamanashi K, Hayashi J, Ishimatsu N, Shimomura O and Kikegawa T 2003 *Solid State Commun.* **127** 573
[17] Farberovich O V 1980 *Sov. Phys.—Solid State* **22** 393
[18] Caldas A, Taft C A and Nazareno H N 1986 *J. Phys. C: Solid State Phys.* **19** 3615
[19] Svane A, Santi G, Szotek Z, Temmerman W M, Strange P, Horne M, Vaitheeswaran G, Kanchana V, Petit L and Winter H 2004 *Phys. Status Solidi* b **241** 3185
[20] Singh D, Rajagopalan M and Bandyopadhyay A K 1999 *Solid State Commun.* **112** 39
[21] Singh D, Rajagopalan M, Husain M and Bandyopadhyay A K 2000 *Solid State Commun.* **115** 323
[22] Singh D, Srivastava V, Rajagopalan M, Husain M and Bandyopadhyay A K 2001 *Phys. Rev.* B **64** 115110
[23] Antonov V N, Harmon B N and Yaresko A N 2002 *Phys. Rev.* B **66** 165208
[24] Vaitheeswaran G, Kanchana V and Rajagopalan M 2002 *J. Alloys Compounds* **336** 46
Vaitheeswaran G, Kanchana V and Rajagopalan M 2002 *Physica* B **315** 64
[25] Rached D, Ameri M, Rabah M, Khenata R, Bouhemadou A, Benkhettou N and Dine el Hannan M 2007 *Phys. Status Solidi* b **244** 1988
[26] Pandit P, Srivastava V, Rajagopalan M and Sanyal S P 2008 *Physica* B **403** 4333
[27] Duan C G, Sabirianov R F, Mei W N, Dowben P A, Jaswal S S and Tsymbal E Y 2007 *J. Phys.: Condens. Matter* **19** 315220
[28] Gupta D C and Kulshrestha S 2009 *Phase Transit.* **82** 240
[29] Perdew J P, Burke K and Ernzerhof M 1996 *Phys. Rev. Lett.* **77** 3865
[30] Trouiller N and Martins J L 1991 *Phys. Rev.* B **43** 1993
[31] Soler J M, Artacho E, Gale J D, Gracia A, Junquera J, Ordejon P and Sanchez-Portal D 2002 *J. Phys.: Condens. Matter* **14** 2745

[32] Murnaghan F D 1944 *Proc. Natl Acad. Sci. USA* **30** 244
[33] Nye J F 1957 *Physical Properties of Crystals, Their Representation by Tensors and Matrices* (New York: Oxford University Press) chapter VIII
[34] Westbrook J H and Fleischer R L (ed) 1995 *Intermetallic Compounds: Principles and Practice* vol 1 (London: Wiley) pp 195–210
[35] Mehl M J, Osburn J E, Papaconstantopoulos D A and Klein B M 1990 *Phys. Rev.* B **41** 10311
Mehl M J, Osburn J E, Papaconstantopoulos D A and Klein B M 1990 *Phys. Rev.* B **42** 5362(E)
[36] Ferrar W L 1941 *Algebra: A Text-Book of Determinants, Matrices and Algebric Forms* (Oxford: Oxford University Press) p 138
[37] Wallace D C 1972 *Thermodynamics of Crystals* (New York: Wiley) chapter 1
[38] Harrison W A 1989 *Electronic Structure and Properties of Solids* (New York: Dover)
[39] Bouhemadou A, Khenata R and Maamache M 2006 *J. Mol. Struct.: Theochem.* **777** 5
[40] Bouhemadou A, Khenata R, Sahnoun M, Baltache H and Kharoubi M 2005 *Physica* B **363** 255